

**(Invited) Directly Silicon-Nitride Waveguide Coupled Ge Photodiode for Non-SOI PIC and Epic Platforms**

S. Lischke<sup>a</sup>, D. Knoll<sup>a</sup>, C. Mai<sup>a</sup>, K. Voigt<sup>b</sup>, A. Hesse<sup>a</sup>, G. Georgieva<sup>b</sup>,  
A. Peczek<sup>c</sup> and L. Zimmermann<sup>a,b</sup>

<sup>a</sup> IHP – Leibniz-Institut für innovative Mikroelektronik, Frankfurt (O.), Germany

<sup>b</sup> Technische Universität Berlin, Institut für Hochfrequenz- und Halbleiter-Systemtechnologien, Berlin, Germany

<sup>c</sup> IHP Solutions GmbH, Frankfurt (O.), Germany

A Ge photodiode, directly coupled to a silicon nitride waveguide, showing more than 67 GHz bandwidth is demonstrated. This paves the way for utterly new SiN waveguide platform based applications. By light feeding through SiN waveguides, the new photodiode can also be a key enabler for a bulk-Si based, monolithically integrated electronic-photonic integrated circuit platform. We show that the new devices, fabricated on bulk-Si, provide the same bandwidths as Si waveguide coupled SOI based reference Ge photodiodes. However, their O-band responsivity is 0.3 A/W, which is about three times lower compared to the SOI waveguide coupled devices. We attribute this effect mainly to substrate leakage, being confirmed by simulations. We demonstrate that bulk-Si based diodes can be fabricated with high yield and low metrics tolerances.

## Introduction

The advance in the areas of cloud infrastructure, mobile communications, high-performance computing, and IOT (Internet of Things) in general leads to a continuous increase of data traffic in all networks. Photonic-electronic integration is a key technology to master traffic growth and therefore an enabler of future network technologies. For some time now, silicon photonic platform technologies are under development. They are considered a key ingredient to solving scaling related issues with photonic-electronic integration of classic photonic technologies. So far, all silicon photonic platforms technologies rely on commercial SOI (silicon on insulator) substrates. SOI substrates are, however, considerably more costly than bulk-silicon wafers. Therefore, the use of bulk silicon as base substrate for silicon photonics would be considered highly advantageous. In recent years there has been intense work on implementing low-loss waveguides (WGs) without the use of SOI, such as silicon-nitride (SiN) based platforms. Despite the demonstrated excellent passive optics a major challenge remaining are high-speed actives such as high-speed modulators and photodetectors (PDs) (1). People have therefore diverted to indirectly coupled active schemes, which allowed the successful demonstration of high-speed detectors and SiN waveguides on the same platform, still making SOI substrates inevitable (2, 3).

In this work we focus on the detector side of a bulk-Si based platform and demonstrate a directly SiN waveguide coupled Ge photo detector with very high opto-electrical (OE)

-3 dB bandwidth of more than 67 GHz (4). Compared to previously demonstrated SiN coupled, bulk-Si located Ge photo detectors (5) our approach offers sufficient performance for upcoming 400 Gbps standards that require 56 Gbd symbol rates. This opens new perspectives for opto-electronic platform technologies such as the following:

- (1) The combination of truly high-speed PDs with SiN WGs could be the start for a novel active SiN platform e.g. aiming at integrated coherent receivers at wavelengths far below the O-band.
- (2) The demonstrated devices are in principle compatible for co-integration with IHP's photonic BiCMOS process (6), which opens various opportunities for novel sensing or spectroscopic applications as well.
- (3) This work could pave the way towards a non-SOI based technology as an alternative to established SOI based PIC or electronic-photonic integrated circuit (ePIC) platforms, e.g. IHP's photonic BiCMOS technology. Circuit fabrication on pure bulk-Si wafers would significantly relieve process complexity, time and thus costs.

### Bulk-Si Photodiode Fabrication

The fabrication of the bulk-Si based, SiN WG coupled Ge PD is to a large extent based on that of the SOI WG coupled reference PD whose fabrication details can be found in (7). For comparison, the SOI based device is shown in Fig. 1a. For this study, neither the actual PD layout was changed, nor were thicknesses of the Ge- or SiN-layers adjusted. All following images and measurement results stem from a 20  $\mu\text{m}$  long Ge PD, the standard device in IHP's ePIC platform. One mandatory adjustment was the replacement of the SOI WG by a bulk-Si region. Both, the SOI based and the SiN WG coupled Ge PDs rely on selective Ge epitaxy on Si. In the bulk-Si case, shallow-trench isolation (STI) regions define the Si-stripe for selective Ge epitaxy, as shown in Fig. 1b.

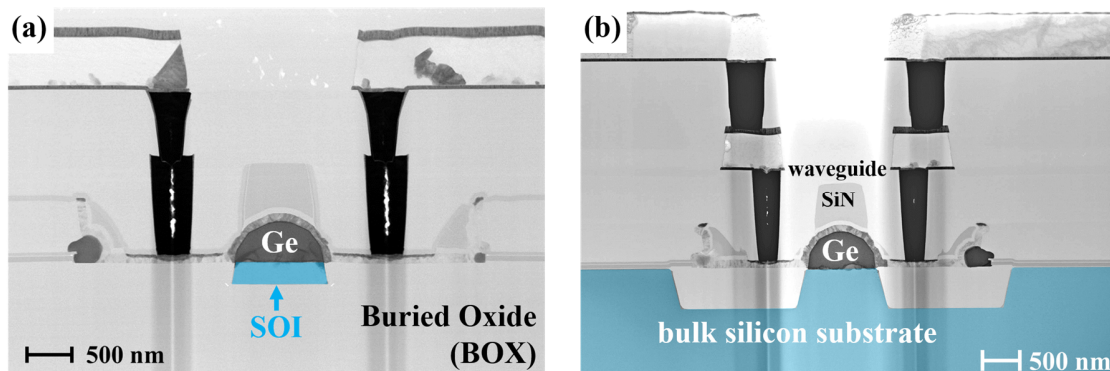


Figure 1: Cross-sections (perpendicular to the light incidence direction) of (a) reference Ge PD fabricated on SOI substrate where selective Ge epitaxy is performed on a SOI WG and (b) Ge PD on bulk-Si where selective Ge epitaxy is enabled by shallow-trench regions. The basic fabrication scheme of the SOI-waveguide Ge PD is maintained. Note that for the sake of image details, the scale is slightly different for both cross-sections.

The Ge PD discussed here has a lateral p-i-n structure where the SiN pedestal located on top of the Ge body supports the definition of the i-region by enabling self-alignment for the ion-implantations applied to form the p- and n-regions. To realize an in-plane waveguide in the non-SOI platform, the SiN pedestal was simply extended to the outside

of the PD region. Hence, SiN WG fabrication does not require an extra photo-mask. Schematic sketches for the bulk-Si and SOI based layouts are presented in Fig. 2.

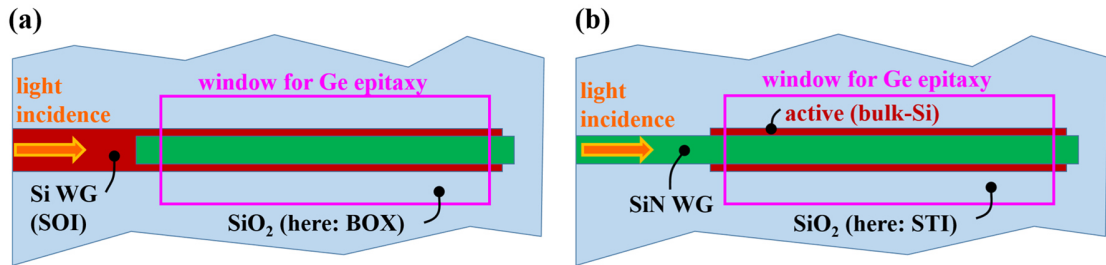


Figure 2: Schematic layout top view of (a) SOI based and (b) bulk-Si Ge PD. Main difference is the replacement of the waveguide layer by active and the extension of the SiN stripe from the diode region (defined by Ge epitaxy window) to the outside to form a SiN waveguide.

Gratings were deployed for fiber-to-chip coupling. SEM cross-sections of a grating coupler and the extended SiN stripe used as WG are shown in Fig. 3. To minimize optical losses due to substrate leakage, the SiN WG is positioned over STI regions. As a minor adjustment, we introduced a CMP step after the deposition of the SiN layer, in order to reduce the surface roughness. Considerable adjustments were done in the contact scheme below the first metal layer (Met1), to avoid abrasion of the SiN WGs during the interlayer dielectrics CMP. The difference can be seen in Figs. 1 (a) and (b).

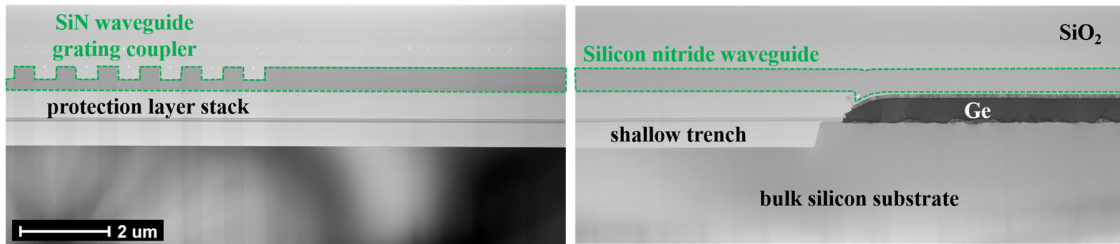


Figure 3: Cross-section (longitudinal) of SiN WG grating coupler (left) and Ge photodiode (right). The SiN waveguide is positioned on top of the protection layer stack required for the photodiode fabrication. Beneath the protection layer, there is shallow-trench region.

### Measurement Results and Discussion

Normalized OE frequency response, measured with a 67 GHz lightwave component analyzer (LCA), of two bulk-Si PDs under zero-bias as well as reverse biases of 1 and 2 V is shown in Fig. 4.

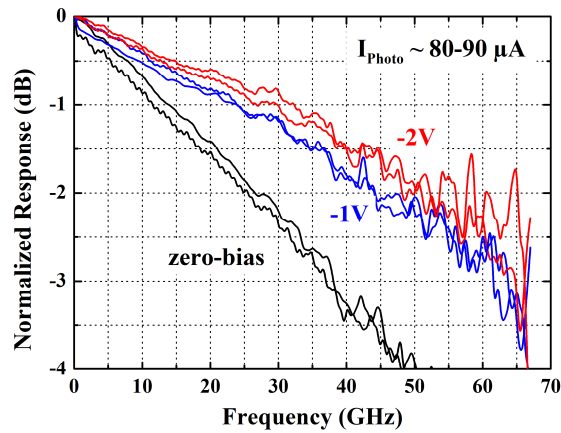


Figure 4: Normalized OE frequency response of two bulk-Si, SiN WG coupled Ge PD measured with a 67 GHz lightwave component analyzer.

Obviously, the new devices exhibit very high -3 dB bandwidths of nearly 40 GHz at zero bias and more than 67 GHz under 2 V reverse bias. This performance is very close to that of the SOI based reference PD (7), despite slightly increased capacitances (Fig. 5), which are probably caused by the fringing field in the bulk-Si.

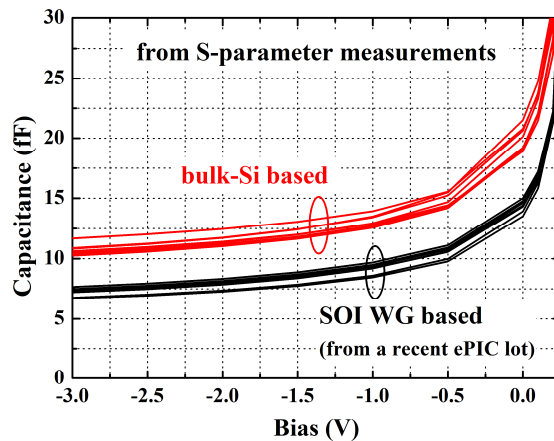


Figure 5: Capacitance vs. voltage characteristics of bulk-Si Ge PDs and SOI based devices, each of both measured on 9 sites of one respective wafer.

Fig. 6 (a) proves identical dark-current behavior of bulk-Si PDs and an SOI based reference device while the photo-currents for different optical input powers at fiber are end shown in Fig. 6 (b).

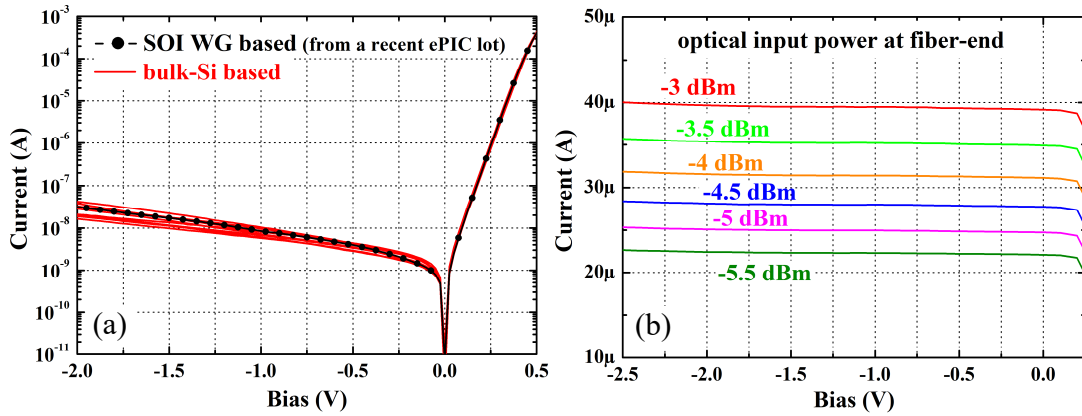


Figure 6: (a) Room temperature dark-current characteristics of bulk-Si Ge PDs, measured on 9 sites of one wafer, and one SOI based reference device and (b) photo-currents of a SiN WG coupled Ge PD at 1310 nm wavelength for different optical input powers. Considering -6.25 dB grating coupler losses, the internal responsivity is about 0.29 A/W.

The internal responsivity is estimated under consideration of the normalized transmission spectra of two grating couplers that are shown in Fig. 7 (a). Note that the maxima of the grating coupler spectra are slightly red shifted (maxima at about 1325 nm). With a loss per grating coupler of about 6.25 dB at 1310 nm, an internal responsivity of 0.29 A/W is determined. Compared to the responsivity of SOI based reference Ge PDs, this value is about three times lower.

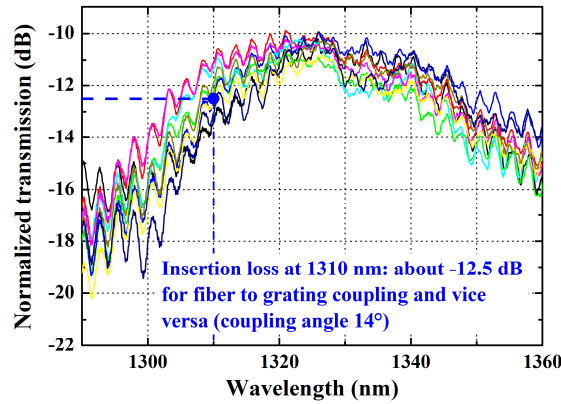


Figure 7: Grating coupler transmission spectra (fiber to grating and vice versa) for 9 sites on one wafer. Insertion loss of one grating coupler is about -6 to -6.5 dB at 1310 nm wavelength. The maxima are slightly red-shifted.

We mainly attribute this responsivity reduction to substrate leakage by radiation modes which can be confirmed by simulations. For investigation of the light propagation in the photodiode, we used a complex mode solver and propagation tools of a commercially available software (8). We recorded the absorption of light by the Ge as well as the substrate leakage over the length of the photodiode, as shown in the following figures. Assumed were two cases: strong absorption (absorption coefficient  $\alpha_{Ge} = 6000 \text{ cm}^{-1}$  at  $\lambda = 1310 \text{ nm}$  for Ge on Si from (9) and without any absorption in the Ge layer ( $\alpha_{Ge} = 0 \text{ cm}^{-1}$ ), which, as an fictitious case, allows for an absorption-independent evaluation of the leakage into the Si-substrate.

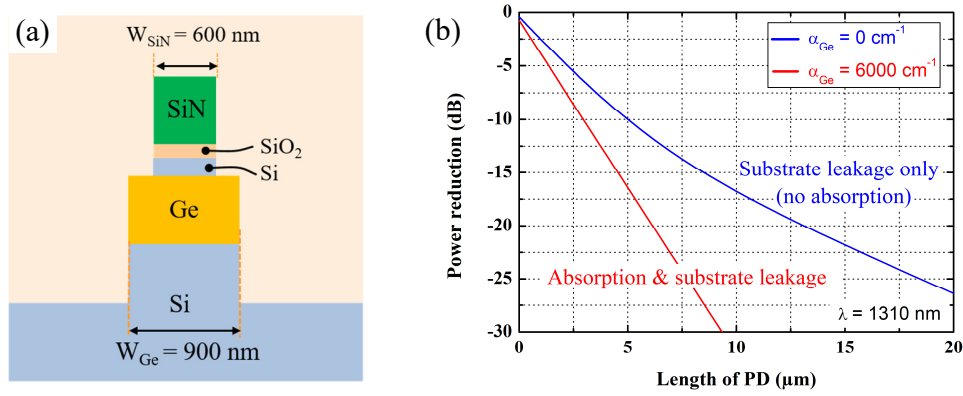


Figure 8: (a) Schematic cross-section of the simulated structure (for the sake of simplification the round-shaped structures were replaced by rectangular shapes) and (b) simulated power reduction versus the length of the Ge structure.

Substantial leakage into the substrate is caused by radiation modes that are formed through the proximity of the Si-substrate, which becomes apparent in Figure 9 showing the light propagation in z-direction for both mentioned cases: (a) without any absorption and (b) for strong absorption in the Ge layer.

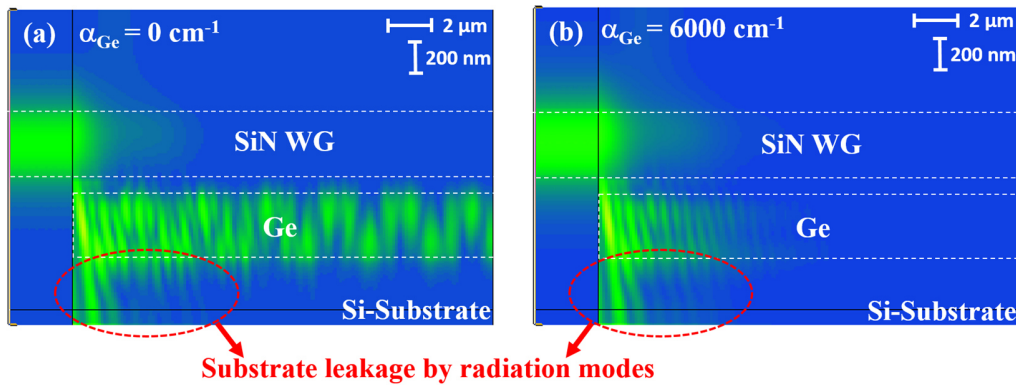


Figure 9: Simulation of light propagation in z-direction (intensity along the waveguide) for (a) no absorption in the Ge-layer (fictitious case  $\alpha_{Ge} = 0 \text{ cm}^{-1}$ ) and (b) for strong absorption in the Ge-layer ( $\alpha_{Ge} = 6000 \text{ cm}^{-1}$ ), ( $\lambda = 1310 \text{ nm}$ ).

The simulation demonstrates that there is a significant leakage into the Si-substrate which qualitatively explains the reduced responsivity of the bulk-Si based Ge PDs. Unfortunately, we only see small potential to improve the responsivity of our bulk-Si based photo detectors by technological or design optimizations, i.e. increase of the Ge layer thickness, without compromising their bandwidth too much.

An overview of SiN platform integrated Ge PDs, compared to a state-of-the-art SOI based Ge PD, is given in Table 1. It makes obvious that our new devices clearly outperform other SiN coupled PDs in bandwidth and dark-current behavior, while there is a clear deficit in responsivity.

**TABLE 1.** Overview of Ge photodiodes available in SiN WG platforms showing a comparison of the -3 dB OE bandwidths, the internal responsivities in O- and C-bands, if applicable, and the diode dark currents. Values in brackets indicate the respective bias conditions. (n/a = values not available in original publication).

Platform Parameter	SOI WGs (7)	SiN on SOI WGs (10)	SiN on SOI WGs (3)	Bulk-Si with SiN WG (5)	Bulk-Si with SiN WG (4), (this work)
<b>OE -3 dB bandwidth</b>	> 67 GHz (-2 V)	29 GHz (-2 V)	> 60 GHz (-1V)	7.2 GHz (-1 V)	> 67 GHz (-2 V)
<b>Internal responsivity in O-band</b>	> 0.8 A/W (-2 V)	0.85 A/W (-2 V)	1A/W (-1V)	<i>n/a</i>	0.3 A/W (-2 V)
<b>Internal responsivity in C-band</b>	> 0.8 A/W (-2 V)	<i>n/a</i>	<i>n/a</i>	> 1 A/W (-1 V)	<i>n/a</i>
<b>dark-current</b>	< 400 nA (-2 V)	2 $\mu$ A (-2 V)	20 nA (-1V)	$\sim$ 1 $\mu$ A (-1 V)	< 400 nA (-2 V)

Transmission spectra of 5 cm long SiN WGs are shown in Fig. 10. The propagation loss of the SiN WG realized only by the extension of the SiN stripe from the Ge PD yields to about 2.3 dB/cm at 1310 nm. We see improvement potential too, e.g. by geometry optimization or introduction of rib-WGs, which could be realized without extra effort using the grating coupler mask and etch.

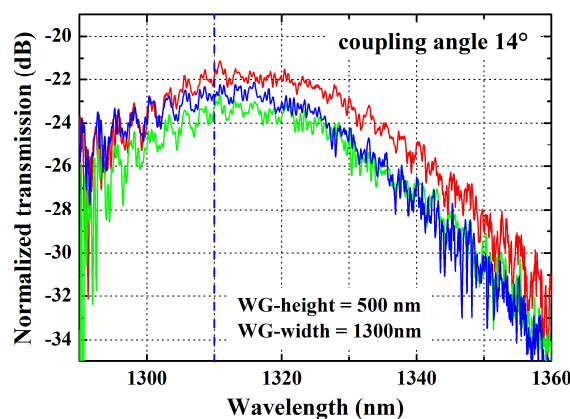


Figure 10: Transmission spectra of 5 cm long SiN WG measured on 3 sites of one wafer. Subtraction of two grating couplers (in and out coupling loss of  $\sim$ 12.5 dB) yields in propagation loss of about 2.3 dB/cm.

That, despite all technological adjustments, the new, bulk-Si based Ge PDs can be fabricated with high yield and low metrics tolerances is demonstrated next. We focus on full-wafer measurements (@ 57 wafer sites) of arrays consisting of 500 Ge PDs contacted in parallel, i.e. 28k diodes are considered in total. Figs. 11 (a) and Fig 12 (a) show the dark-current behavior of the arrays for reverse bias of 1 V and 2 V, respectively. Under reverse bias of 2 V, only 3 of 57 arrays located at the wafer edge failed. Corresponding cumulative plots are shown in Fig. 11 (b) and Fig. 12 (b), respectively.

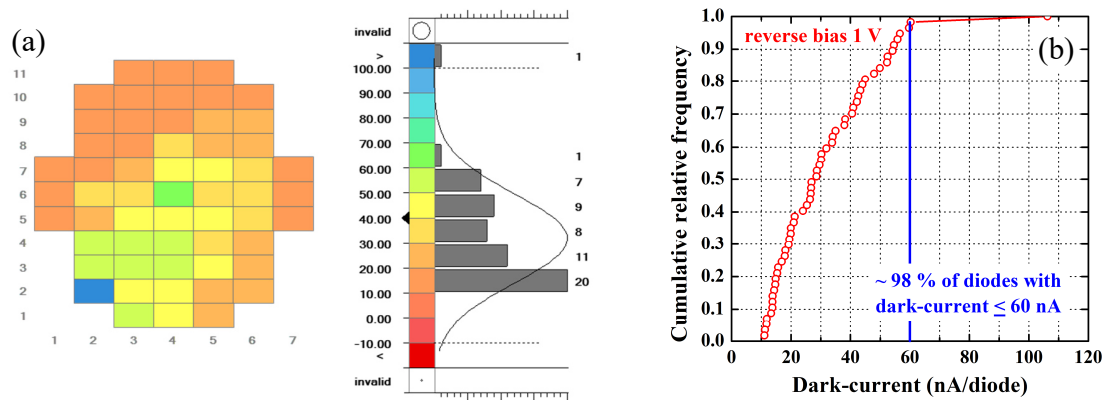


Figure 11: (a) Wafermap and histogram of dark-currents (nA per single diode) at a bias of -1 V of Ge PD arrays consisting of 500 diodes in parallel, measured on 57 wafer sites and (b) corresponding cumulative plot (nA per single diode).

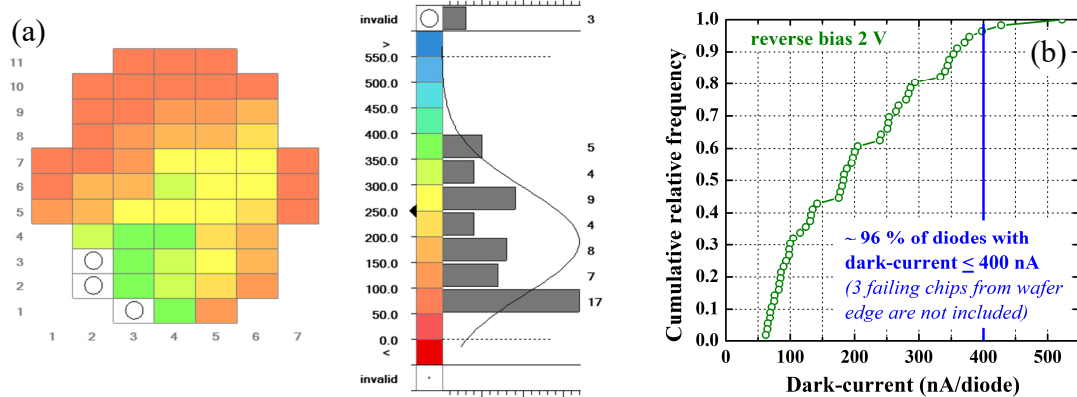


Figure 12: Wafermap and histogram of dark-currents (nA per single diode) at a bias of -2 V of Ge PD arrays consisting of 500 diodes in parallel, measured on 57 wafer sites and (b) corresponding cumulative plot (nA per single diode).

Fig. 13 (a) shows a wafermap with histogram of the forward-currents of the Ge PD arrays at a bias of 0.2 V, while the corresponding cumulative plot is shown in Fig. 13 (b).

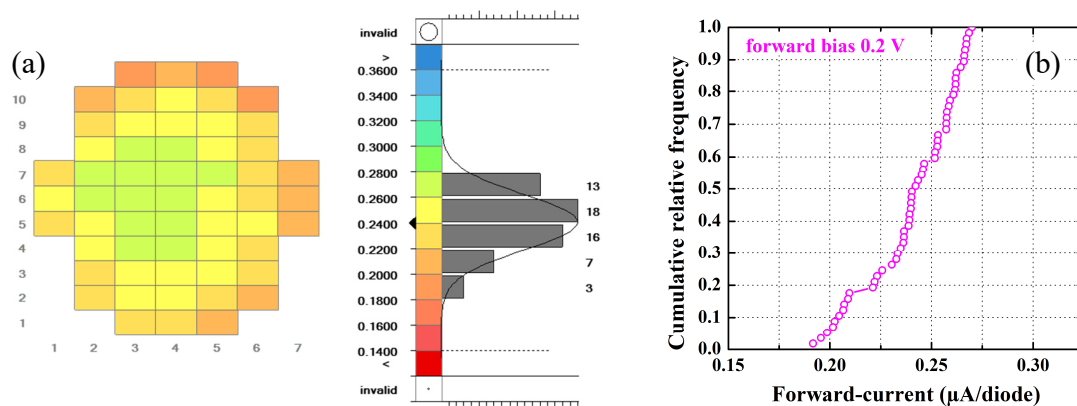


Figure 13: Wafermap and histogram of forward-currents ( $\mu\text{A}$  per single diode) at a bias of 0.2 V of Ge PD arrays consisting of 500 diodes in parallel, measured on 57 wafer sites and (b) corresponding cumulative plot ( $\mu\text{A}$  per single diode).

Results of a follow up lot with slightly deeper etched gratings to reduce the red-shift demonstrate loss mean values of about 5 dB per coupler at 1310 nm (Fig. 14). This clearly reflects also a homogeneous SiN WG and coupler fabrication.

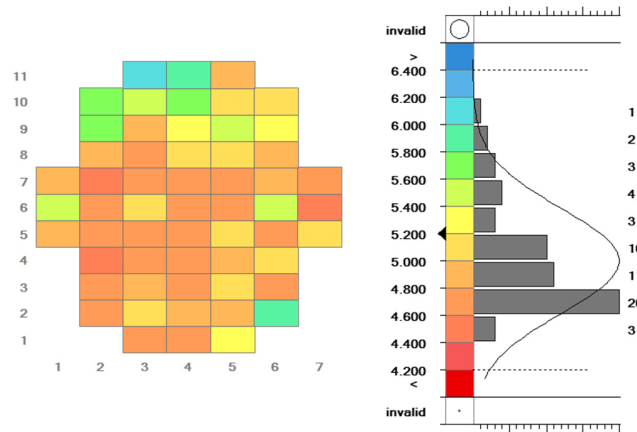


Figure 14: Wafermap and histogram of grating coupler insertion losses at 1310 nm (in dB, coupling angle  $14^\circ$ ), determined for 57 sites of a follow up wafer with compensated red shift, compared to Fig. 7.

The facts that the SiN coupled Ge PD fabrication scheme largely complies with that of the reference SOI based devices and that no additional thermal budget is applied for the SiN WG fabrication facilitate the implementation into IHP's photonic BiCMOS process. Together with substrate independent modulator approaches like recently demonstrated BTO based devices (11), the SiN coupled PD presented in this work could pave the way for utterly new high speed SiN based PIC or ePIC platforms with various opportunities for new applications.

## Conclusion

We have demonstrated for the first time a Ge photodiode, directly coupled to a SiN waveguide, with more than 67 GHz bandwidth. This unique combination and the potential integration with high-speed electronics could pave the way for an utterly novel SiN platform potentially addressing applications in sensors, spectroscopy or even Tele- and Datacom. By simulations we showed that the responsivity of the bulk-Si based Ge PDs, which is lower compared to that of SOI based reference and other SiN coupled devices, is caused by leakage into the Si-substrate. We further demonstrated that bulk-Si based diodes can be fabricated with high yield and low metrics tolerances.

## Acknowledgment

The authors gratefully acknowledge support from IHP's cleanroom staff and funding by German Ministry of Research and Education (BMBF), projects SPEED and PEARLS, as well as support by European Commission, projects DIMENSION and plaCMOS.

## References

1. P. Muñoz, G. Micó, L. A. Bru, D. Pastor, D. Pérez, J. D. Doménech, J. Fernández, R. Baños, B. Gargallo, R. Alemany, A. M. Sánchez, J. M. Cirera, R. Mas and C. Domínguez, *Sensors (Basel, Switzerland)*, **17**(9) (2017).
2. W. D. Sacher, Y. Huang, G.-Q. Lo and J. K. S. Poon, *J. Lightwave Technol.*, **33**(4), 901–910 (2015).
3. F. Boeuf, A. Fincato, L. Maggi, J. F. Carpentier, P. Le Maitre, M. Shaw, S. Cremer, N. Vulliet, C. Baudot, S. Monfray, S. Jan, C. Deglise, J. R. Manouvrier, C. Durand, A. Simbula, D. Goguet, P. Bar, D. Ristoiu, F. Leverd, L. Babaud, A. Daverio, M. Binda, A. Bazzotti, A. Canciamilla, L. Ramini, M. Traldi and P. Gambini, in *2019 IEEE International Electron Devices Meeting (IEDM)*, 33.1.1-33.1.4, IEEE (07.12.19 - 11.12.19).
4. S. Lischke, D. Knoll, C. Mai, A. Hesse, G. Georgieva, A. Peczek, A. Kroh, M. Lisker, D. Schmidt, M. Fraschke, H. Richter, A. Kruger, U. Saarow, P. Heinrich, G. Winzer, K. Schulz, P. Kulse, A. Trusch and L. Zimmermann, in *2019 IEEE International Electron Devices Meeting (IEDM)*, 33.2.1-33.2.4, IEEE (07.12.19 - 11.12.19).
5. D. Ahn, C.-Y. Hong, J. Liu, W. Giziewicz, M. Beals, L. C. Kimerling, J. Michel, J. Chen and F. X. Kärtner, *Optics express*, **15**(7), 3916–3921 (2007).
6. D. Knoll, S. Lischke, A. Awny and L. Zimmermann, *ECS Transactions*, **75**(8), 121–139 (2016).
7. S. Lischke, D. Knoll, C. Mai, L. Zimmermann, A. Peczek, M. Kroh, A. Trusch, E. Krune, K. Voigt and A. Mai, *Optics express*, **23**(21), 27213–27220 (2015).
8. *Optical Propagation Software using EigenMode Expansion (EME) - FIMMPROP*, <https://www.photond.com/products/fimmprop.htm> (2020-04-07T13:08:57.000Z).
9. V. Sorianello, A. Perna, L. Colace, G. Assanto, H. C. Luan and L. C. Kimerling, *Appl. Phys. Lett.*, **93**(11), 111115 (2008).
10. W. D. Sacher, J. C. Mikkelsen, Y. Huang, J. C. C. Mak, Z. Yong, X. Luo, Y. Li, P. Dumais, J. Jiang, D. Goodwill, E. Bernier, P. G.-Q. Lo and J. K. S. Poon, *Proc. IEEE*, **106**(12), 2232–2245 (2018).
11. F. Eltes, M. Kroh, D. Caimi, C. Mai, Y. Popoff, G. Winzer, D. Petousi, S. Lischke, J. E. Ortmann, L. Czornomaz, L. Zimmermann, J. Fompeyrine and S. Abel, in *2017 IEEE International Electron Devices 2017*, 24.5.1-24.5.4.